# Contributions to Low-Cost, Nonresonant Electronic Ballasts

Pedro S. Almeida; Anderson P. Silva and Henrique A. C. Braga, *Senior Member, IEEE*
*NIMO – Núcleo de Iluminação Moderna*
*UFJF – Universidade Federal de Juiz de Fora*
pedro.almeida@engenharia.ufjf.br; henrique.braga@ufjf.edu.br

*Abstract*- **The aim of this paper is to revisit the theme of non-resonant electronic ballasts focusing on a specific topology introduced in the last few years. Its complete mathematical analysis, which has not been fully explored in the past, and its practical implementation as a dc-fed electronic ballast unit is provided. The ballast here presented was successfully prototyped and is capable of pre-heating, igniting and driving two or more fluorescent light bulbs in series and has intrinsic protection against broken filaments and lamp absence. Furthermore, it relies solely on a single power switch and a relatively small-sized inductor per lamp, plus simple op-amp based control circuitry. An external protection circuitry is also presented in this paper, for protecting the power switch against lamp faulty conditions.**

## I.    INTRODUCTION

Non-resonant inverter based electronic ballasts have recently found their way into lighting systems as a cheaper alternative [1], [2], [3], [4], [6] to the usual half-bridge resonant inverter (on a low power basis) or as quasi-square wave ballasts to feed HID lamps, thus reducing acoustic resonances [8], [11].

From the cost point of view, it is desirable for an electronic ballast to have as few power components, filters and control circuitry as possible [3]. The single-switch ballast arises from these premises, in an attempt to lower lighting costs without losing the advantages of high frequency operation [7], [10].

Also, the proposed ballast (Fig. 1) can be easily employed to series fluorescent lighting [1], [2]. All these characteristics, together with the proposed DC bus connected to a main dedicated rectifier, can further lower the cost of the whole system and still maintain efficiency.

Though the idea of such a low cost and simple system is very attractive, the lack of precise modeling or further mathematical detailing on previous works led to experimental deviations from theoretical model, mainly due to oversimplified analysis [1], [2]. Waveform asymmetry, power fluctuations, high lamp current crest factor, operating point imprecision and very high filament current during normal operation were some of the main drawbacks of these studies.

Willing to improve experimental results and to apply the topology on the proposed low cost series fluorescent DC lighting system, a more accurate mathematical analysis was developed, resulting also in a good design methodology. Moreover, a close to a commercial unit approach has also motivated this work.

Experimental results for a complete prototype, designed by using the method here presented, are included, feeding two high-efficiency fluorescent T-8 32W bulbs.

## II.    PROPOSED TOPOLOGY AND CONTROL STRATEGY

Fig. 1 depicts the proposed inverter topology. This single switch inverter has been named a "buck-boost inverter" [4], [8], as it can be derived from the referred DC-DC converter by removing its diode. The lamps are associated in series with the switch.

A current mode control strategy was successfully employed on past prototypes [1], [2], [3], [4] and stems on preventing the current on the switch to go higher than a reference value, $i_M$. When this happens, the control circuitry opens the switch and holds it that way for a pre-determined amount of time, named $t_o$. The simple control circuitry can be implemented using a dual open-collector comparators IC, as Fig. 2 shows. Points x and y are the interface with the protection circuit, as described in Section III. Voltage $V_{cc}$ is the control circuit power supply provided by means of the same rectifier that generates $2V_B$.

Thus, the complete ballast stage comprises only one power MOSFET, two inductors (for driving two fluorescent bulbs), one cheap IC and very few additional low power elements.
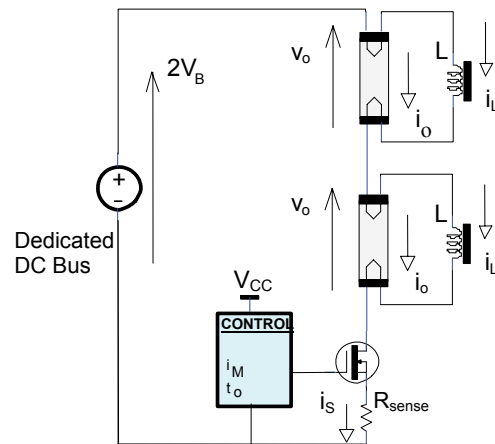


Fig. 1.  Proposed topology of the single switch non-resonant (SSNR) ballast and lamp series association.
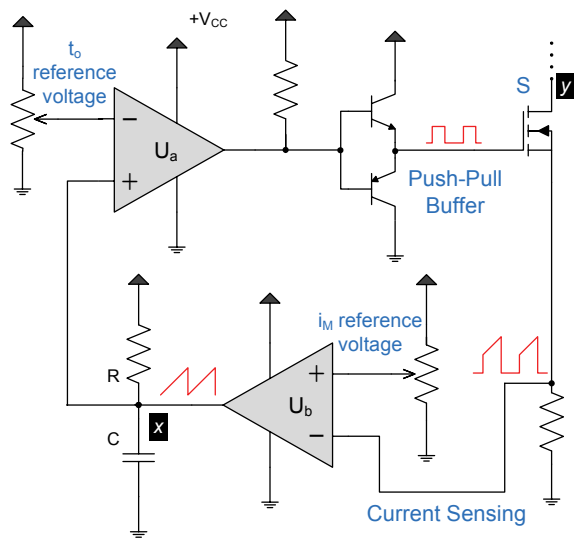
Fig. 2. Current-mode control circuitry and steady-state working principle.

## III. IGNITION PROCESS AND PROTECTION SYSTEM

The process of igniting the lamp relies on the avalanche behavior of the power MOSFET. This happens when a current is forced through the open switch, and a reverse voltage up to 30% (typically) greater than the rated drain-source voltage of the device appears [2]. This is exactly what happens when the lamp has not yet ignited, and the MOSFET is forced into unclamped inductive switching (UIS). These devices can indeed withstand repetitive avalanche events during ignition [9].

Supposing the lamp has infinite resistance when turned off, the current that flows through the switch is the same that flows through the inductors and lamp electrodes. This causes these filaments to be pre-heated, thus reducing the required strike voltage and accelerating the ignition process.

Supposing it discharges completely at the end of every cycle, the inductor current at this situation is given by (1). When the current through the switch rises above the threshold set by the control circuitry, it opens and its UIS operation forces the avalanche, producing a negative voltage spike, of magnitude given by (2), that appears divided across each lamp, during almost all the time the switch is held open.

$$i_S(t) = i_L(t) = \frac{V_B}{L} t \, ,$$
$$\text{until } t = t_1 = \frac{L}{V_B} i_M \tag{1}$$

Where:
$i_S$ – switch current
$i_L$ – inductor current
$i_M$ – maximum switch
 current (from control)

L – inductance of parallel
 inductor
$V_B$ – bus voltage divided across
 each lamp

$$v_o(t) = V_B - \frac{V_Z}{n} \, ,$$
$$\text{until } t = t_1 + t_o = \frac{L}{V_B} i_M + t_o \tag{2}$$

Where:
$v_o$ – voltage across one lamp
$V_Z$ – avalanche breakdown
 voltage of switch

n – number of lamps in
 series association
$t_o$ – switch-off interval
 (from control, Fig. 2)

The lamp filament pre-heating and sub sequential high voltage spikes are enough to strike the bulb arc and start the steady state operation of the ballast.

Although the topology presents intrinsic protection against broken filament or lamp absence [3], a broken or faulty lamp with intact filaments could force the inverter to attempt ignition continuously, with probable destruction of the power switch due to endless repetitive avalanche breakdown cycles. Therefore, protection against this scenario is obviously important if one intends to employ such ballast within the lighting system proposed.

The protection circuitry here proposed is shown in Fig. 3. It comprises a selective peak detector that should inhibit ignition process after a determined amount of trials that have been unsuccessful in the attempt to strike an arc.

The resistive divider network placed at the drain of the MOSFET steps down the drain voltage, to the point where the series DIAC will only conduct if this voltage is above a certain level. This only happens during successive ignition attempts, causing the capacitor of the protection circuit to charge and eventually trigger the second DIAC and the SCR gate, if steady state is not achieved within a certain amount of time. Then the switch is told to be held open as long as there is power applied to the ballast (SCR is latched), because the voltage at the second comparator ($U_b$) output goes down to nearly zero.
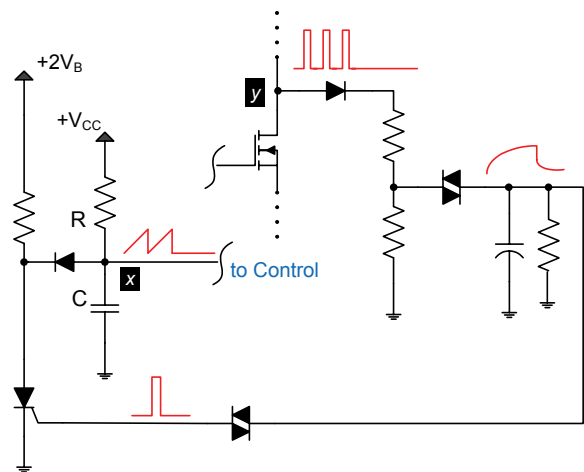


Fig. 3. Protection circuitry and working principle during faulty ignition. Complete control circuit is not shown (only the RC network that defines $t_o$).
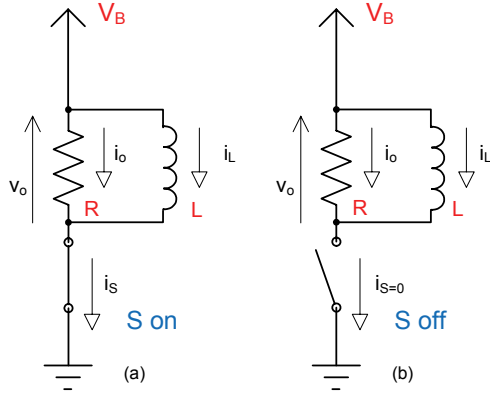
Fig. 4. Inverter equivalent circuit and operation:
(a) positive half-cycle, (b) negative half-cycle.

If the bulbs ignite before protection circuit triggers the SCR, then steady-state is achieved and the voltage spikes at the drain of the MOSFET become much smaller than at ignition. So, the first DIAC stops conducting and also stops charging the capacitor, which now discharges through a parallel resistor. It's a relatively simple and effective protection circuitry.

## IV.    MATHEMATICAL ANALYSIS OF INVERTER

Since the inverter is very simple and comprises only one reactive element (the inductor), the mathematical analysis could be made in time domain, solving the first order ODEs for both switch-closed and switch-opened states. These two states are depicted at Fig. 4.

Replacing the lamp for its equivalent resistance at operating point (R) and assuming CCM operation, (3) to (8) arise.

*(a) Positive half-cycle ($0 \leq t \leq t_1$):*

$$i_L(t) = I_1 + \frac{V_B}{L}t \tag{3}$$

$$i_o(t) = \frac{V_B}{R} \tag{4}$$

$$i_S(t) = \frac{V_B}{R} + \frac{V_B}{L}t + I_1 \tag{5}$$

Where:
$I_1$ – maximum inductor current

*(b) Negative half-cycle ($t_1 \leq t \leq T$):*

$$i_L(t) = I_2 e^{\frac{-(t-t_1)}{\tau}} \tag{6}$$

$$i_o(t) = -i_L(t) \tag{7}$$

$$i_S(t) = 0 \tag{8}$$

Where:
$I_2$ – minimum inductor current        $\tau = \dfrac{L}{R}$ – time constant
$t_1$ – switch-on time

These equations suggest the theoretical waveforms of Fig. 5.

Equations (9) and (10) relate the maximum and minimum inductor current (due to current continuity), while (11) gives the time the switch is held closed, $t_1$. All these are now set as functions of the equivalent lamp resistance (R) and input controllable variables, i.e., the bus voltage for each lamp ($V_B$), the inductance (L), the maximum switch current ($i_M$) and the switch-off time ($t_o$).

$$I_2 = i_M - \frac{V_B}{R} \tag{9}$$

$$I_1 = I_2 e^{\frac{-t_o}{\tau}} \tag{10}$$

$$t_1 = \frac{L}{V_B}\left(i_M - \frac{V_B}{R}\right)\left(1 - e^{\frac{-t_o}{\tau}}\right) \tag{11}$$

Using (11) and $t_o$ for writing the duty cycle (d) and frequency of operation (f) results in (12) and (13), respectively, where $T = t_1 + t_o$ is the period of operation.

$$d = \frac{t_1}{T} = \frac{t_1}{t_1 + t_o} \tag{12}$$

$$f = \frac{1}{T} = \frac{1}{t_1 + t_o} \tag{13}$$

Altogether, these set of equations can be manipulated to find the average power delivered to the lamp, resulting in (14).

$$P(R) = \frac{V_B^2}{R}d + \frac{R.\tau}{2T}(1 - e^{\frac{-2t_o}{\tau}})\left(i_M - \frac{V_B}{R}\right)^2 \tag{14}$$
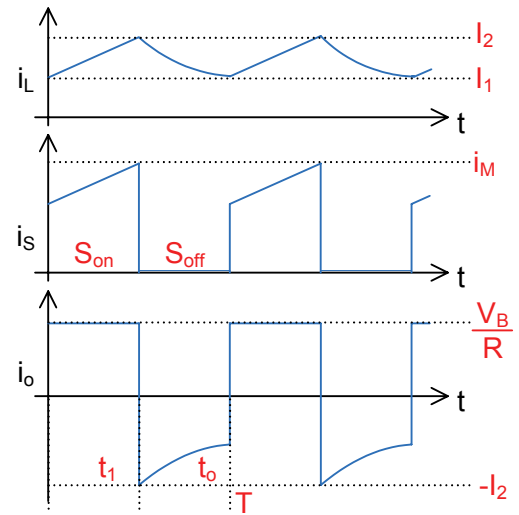


Fig. 5. Theoretical waveforms predicted for the non-resonant inverter.

To find the operating point of both ballast and lamp, one should plot (14) against the equivalent lamp resistance versus lamp power characteristic curve, $P_L(R)$. This characteristic can be obtained experimentally for the fluorescent bulb chosen.

## V.  LAMP CURRENT AND CREST FACTOR

Though past works [1], [2], [3] did not show much concern in predicting precisely the lamp current crest factor (CF) and lamp current asymmetry, it was suggest that the present work should include means of calculating and improving both CF and the symmetry of lamp current.

Therefore, (15) and (16) can be employed for predicting the lamp current CF, depending on the peak current (conditions shown). These equations come to provide further aid when designing and implementing a practical ballast circuit.

$$CF = \frac{Ri_M - V_B}{R\sqrt{\frac{V_B^2}{R^2}d + \frac{\tau}{2T}(1-e^{-2t_o/\tau})\left(i_M - \frac{V_B}{R}\right)^2}} \quad (15)$$

$$\text{if} \quad 2\frac{V_B}{R} \le i_M$$

$$CF = \frac{V_B}{R\sqrt{\frac{V_B^2}{R^2}d + \frac{\tau}{2T}(1-e^{-2t_o/\tau})\left(i_M - \frac{V_B}{R}\right)^2}} \quad (16)$$

$$\text{if} \quad 2\frac{V_B}{R} \ge i_M$$

It is suggested that the CF should be kept below 1.7 [5], [7], even at non-sinusoidal waveforms, since higher values can decrease lamp lifespan and cause lamp-end darkening [6].

As for the current asymmetry, for it to be kept low, it is here suggested that the ballast should work at a duty cycle as close to 50% as possible, with no average value whatsoever. The average value of voltage across the lamp must be zero, since it is also the voltage across the inductor. This leads to current average value being virtually zero also, since we are using an equivalent resistance model for the lamp, which is fairly true at high frequencies [7], [10]. Thus, the areas under each current half-cycle are equal.

## VI.  LAMP MODELING AND CHARACTERISTIC CURVE

For finding the operating point of the ballast, it is necessary to find the intersection point between the lamp and inverter characteristic curves, rather than assuming that its equivalent resistance is already known (e.g., it is operated at rated power and voltage, thus $R = V^2/P$).
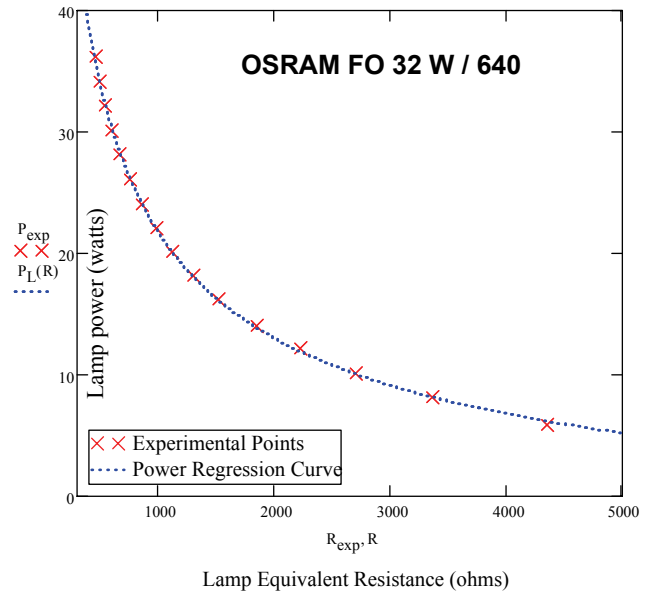


Fig. 6.  Experimental data from the 32W fluorescent bulb and curve fitting.

From varying the power delivered to an OSRAM FO32W/640 T8 fluorescent bulb at high frequency, experimental points can be obtained and fitted into a curve. In this particular case, a power regression was used for finding the equation that describes the lamp power as function of its equivalent resistance. The resulting characteristic curve is shown in Fig. 6 and its equation is given by (17).

$$P_L(R) = aR^b + c, \quad (17)$$

on which

$$a = 907.303 \text{ W}.\Omega^{-1} \quad (17.a)$$

$$b = -0.492 \quad (17.b)$$

$$c = -8.614 \text{ W} \quad (17.c)$$

## VII.  DESIGN METHODOLOGY AND PRACTICAL EXAMPLE

For the design of a SSNR ballast, the operating point must be found by the intersection point $P_L(R) = P(R)$. Using the mathematical modeling here presented, it is possible to iterate the values for $i_M$ and $t_o$ (controllable variables), for given L and $V_B$ (input variables).

Also, one can choose ranges for frequency, duty cycle and CF in which is desired to operate the ballast. An approximate algorithm for this proposed design method is depicted in Fig. 7.

It was demonstrated that $V_B$ is inversely proportional to the duty cycle, and this last is closely related to the CF. This characteristic is shown by the curve at Fig. 8.

It is also known that larger values for L imply in better CF and lower frequency, but also a larger sized component, while smaller values imply in higher frequency operation for maintaining the same CF, therefore higher switching losses.
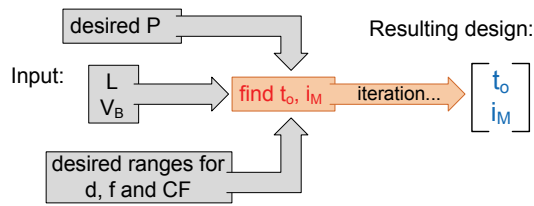
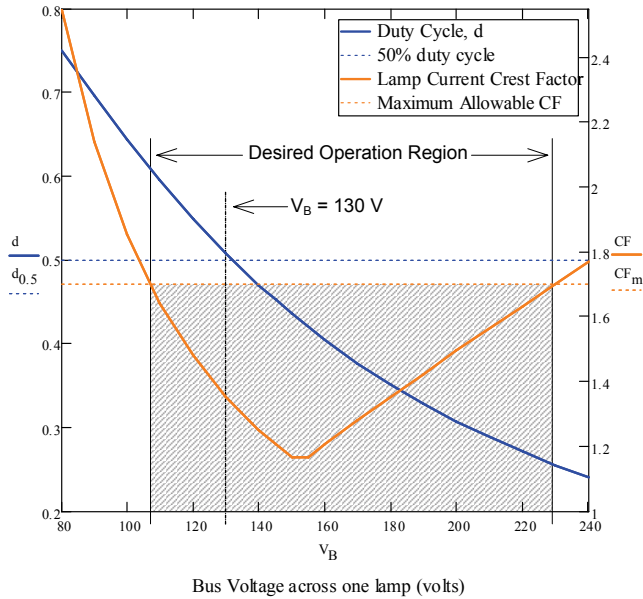Fig. 7. Iterative design method for implementing a prototype.



Bus Voltage across one lamp (volts)

Fig. 8. Duty cycle and crest factor as functions of bus voltage. Desired operation region for CF < 1.7 is shown.



Lamp Equivalent Resistance (ohms)

Fig. 9. Interception of curves at operating point. Power is indicated.

By using the iterative method proposed in Fig. 7 and for a desired output power close to lamp rated power ($P(R) \approx 32$ W), CF smaller than 1.7 and as low as possible, duty cycle as close to 50% as possible (as mentioned before) and restricting the operating frequency between 20 kHz and 70 kHz (to avoid audible noise and high switching losses), a design example was calculated, using $L = 6.6$ mH and $V_B = 130$ V as input variables. As mentioned before, the dc bus voltage could be provided by means of an external high power factor pre-regulator (not shown), which could be used to feed several sets of ballast and lamps. The control circuit supply voltage, $V_{cc}$, is also supposed to be provided by this same front-end regulator.

The resulting design for control parameters was $i_M = 558$ mA and $t_o = 7.4$ μs. The intersection point of lamp and inverter characteristics is shown at Fig. 9, and Table I shows the complete result for this design, from the mathematical modeling and equations presented.

From the curve at Fig. 8, which was drawn using the aforementioned design values, it can be seen that the chosen $V_B$ is within the desired operation region defined and also very close to achieve 50% duty cycle. Therefore, this is a good design that agrees with what was proposed for this ballast operation in Section V.
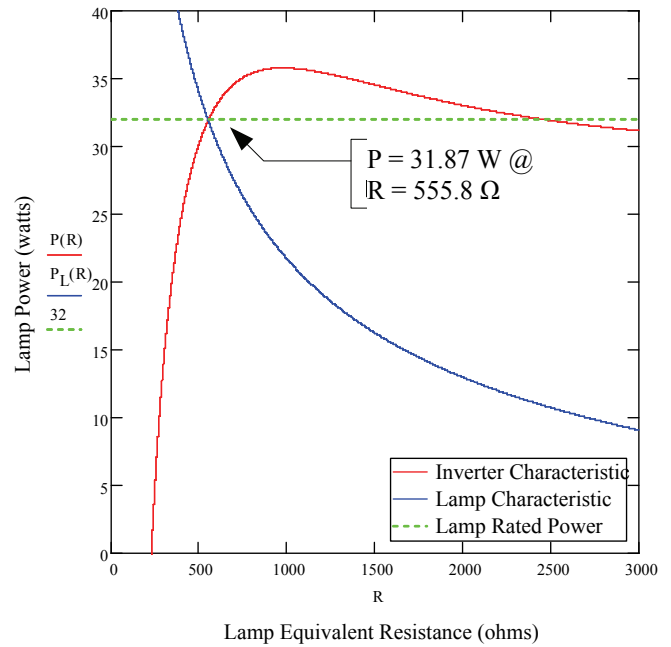
## VIII. EXPERIMENTAL RESULTS

A prototype using the values from the above calculated example (Table I) was built and tested, fed by a DC power supply with negligible voltage ripple. The prototype is shown in Fig. 10 – (a), side by side with a commercial auto-oscillating half-bridge AC-fed resonant ballast. Fig. 10 shows the discrepancy in number of components between these two topologies of ballasts. Though a TOSHIBA 2SK1120 power MOSFET was used, any cheaper repetitive avalanche rated switch (e.g., an IRFBG20) of the same voltage rating (1000 V) but lower current could be easily used, since maximum device current is low. Inductors are small C core type of IP6 material.

TABLE I
PROTOTYPE - EXPECTED VALUES

| SYMBOL | VALUE | DESCRIPTION |
|---|---|---|
| $2 \cdot V_B$ | 260 V | DC Bus Voltage ($V_B = 130$ V at each lamp) |
| L | 6.6 mH | Parallel Inductance |
| $i_M$ | 558 mA | Maximum Switch Current |
| $t_o$ | 7.4 μs | Switch-off Time Interval |
| P | 31.87 W | Output Power (one lamp) |
| R | 555.8 Ω | Equivalent Lamp Resistance |
| d | 50.8 % | Duty Cycle of Current |
| f | 66 kHz | Frequency of Operation |
| CF | 1.35 | Lamp Current Crest Factor |
| $i_{oRMS}$ | 239 mA | Lamp RMS Current |
| $v_{oRMS}$ | 133 V | Lamp RMS Voltage |
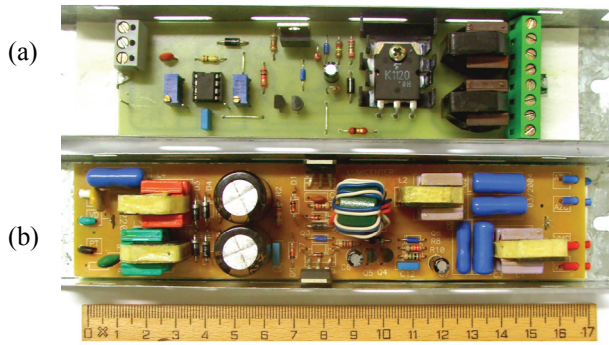
Fig. 10. Comparison between (a) implemented prototype and (b) commercial ballast for two 32 W fluorescent bulbs. (Ruler is in centimeters.)

The experimental results obtained in the prototype are shown at Table II. Various waveforms of ignition state, protection circuit operation and during steady-state are depicted in Fig. 11 to Fig. 14. Note that the lamp ignites with almost 400V (Fig. 11) and the protection circuit waits nearly 2 seconds to inhibit ignition (Fig. 12), in the case of faulty lamp.
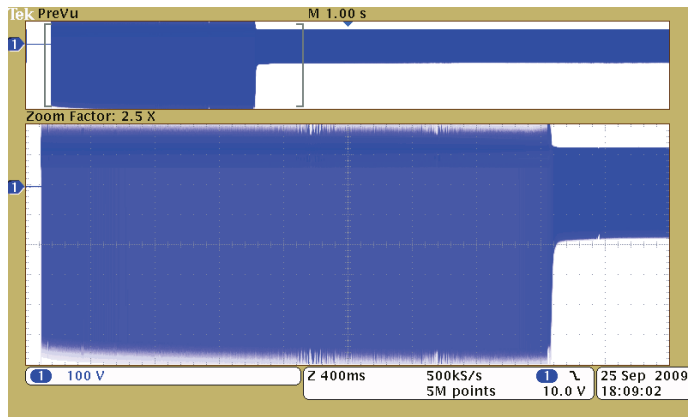


Fig. 11. Lamp voltage at ignition state and transition to steady state. (400ms/div, 100V/div)
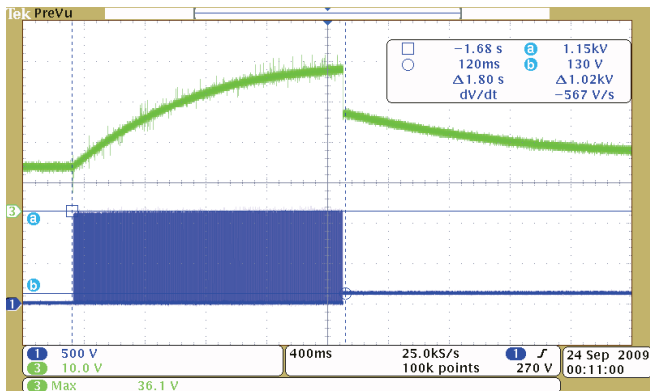


Fig. 12. Bottom trace shows drain voltage (500V/div) during ignition attempt with faulty lamps, showing how the protection circuit inhibits ignition after a number of unsuccessful attempts. Upper trace shows protection circuit capacitor voltage rising (10V/div) and DIAC triggering. (400ms/div)
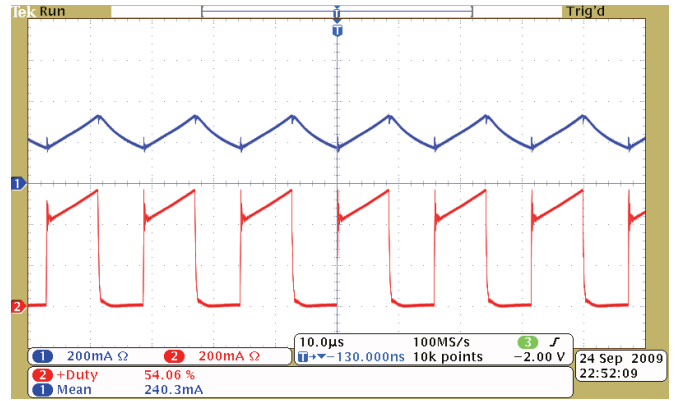


Fig. 13. Upper trace shows inductor current and bottom trace shows switch drain current, all at steady state. (10μs/div, 200mA/div)
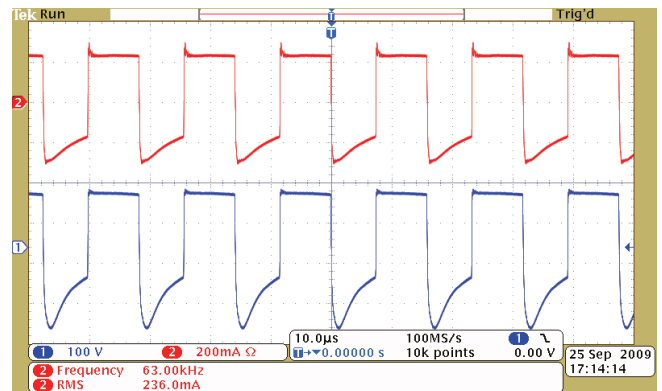


Fig. 14. Upper trace shows lamp steady-state current (200mA/div) and bottom trace shows lamp steady state voltage (100V/div). (10μs/div)

TABLE II
PROTOTYPE – EXPERIMENTAL RESULTS

| SYMBOL | VALUE | DESCRIPTION |
|---|---|---|
| P | 31.85 W | Output Power (one lamp) |
| d | 54.06 % | Duty Cycle of Current |
| f | 63 kHz | Frequency of Operation |
| CF | 1.3 | Lamp Current Crest Factor |
| $i_{oRMS}$ | 236 mA | Lamp RMS Current |
| $v_{oRMS}$ | 134.8 V | Lamp RMS Voltage |
| $I_f$ | 270 mA | RMS Filament Current (estimated from switch current) |

The efficiency of the ballast was measured taking into account also the power consumed by the control circuit. Since it only needs 270 mW, with a ballast output power of approximately 63.7 W and an input power of 69.31 W, the efficiency was calculated as 91.6%.

In spite of featuring simplicity, compactness and a reduced component count, one drawback of the employed topology is that the lamp filament shares, during half a cycle, the relatively high peak current ($i_M$) with the semiconductor switch, though the RMS value for estimated filament current is not very high.

## DISCUSSION AND CONCLUSIONS

This work has presented the complete mathematical analysis and design methodology for implementing a single switch non-resonant electronic ballast, to be applied within a DC-supplied lighting system.

The implemented prototype was designed following the exact proposals of low current asymmetry and very low lamp current crest factor, as well as rated power operation of modern high-efficiency T8 32 W fluorescent bulbs. Lower filament current, high frequency operation, small inductor design and good efficiency were also achieved.

The prototype showed the precision of calculated operating point and the feasibility of its implementation on such low cost lighting system. The experimental results obtained were precise and in good agreement with the theoretical counterparts.

The proposed system is yet intended to be completely built and widely tested, thus a main regulated rectifier with power factor correction (PFC) will be constructed for feeding a high number of ballast units. The results will be presented in future authors' publications.

Comparing the final cost of implementing a high number of ballasts to be used on a wide area, the proposed DC bus plus the SSNR ballast units would result in a cheaper alternative than the present technology of AC-fed resonant ballasts, as the cost of a single rectifier would be diluted by the number of units supplied. This proposal is supported by the fact that producing only one larger rectifier with PFC and low cost inverters is cheaper than producing a number of small rectifiers plus PFC, associated to medium cost inverters inside the ballast unit: above a certain installed load threshold, the cost of a large number of AC-fed ballasts tends to overwhelm the total cost of rectifier plus SSNR ballasts.

Also, another alternative for using the presented SSNR inverter is on on-board applications that already count with DC distributed energy, such as aircrafts, omnibuses, ships etc., emergency UPS supplied lighting or even at the integration of photovoltaic generation and DC lighting.

## REFERENCES

[1] L. S. Mattos, R. N. Marques, C. A. C. Dutra, H. A. C. Braga, "Feasibility Investigation of a DC Lighting System Based on the Series Association of Fluorescent Lamps Driven by Single-Switch Ballasts," *Seminario Anual de Automática, Electrónica Industrial e Instrumentación,* Gijón – Spain, 2006.

[2] L. S. Mattos, R. N. Marques, C. A. C. Dutra, H. A. C. Braga, "An Electronic DC Lighting System Based on Series Association of Fluorescent Lamps and Single-Switch Ballasts," *VII IEEE-Induscon*, Recife - Brazil, 2006.

[3] M. Rico-Secades, E. L. Corominas, J. Ribas, A. J. Calleja, J. M. Alonso, J. Cardesín, "A Low-Cost Electronic Ballast for a 36 W Fluorescent Lamp Based on Current-Mode-Controlled Boost Inverter: Design Example for a Greenhouse Application with a 120 DC Bus Power Distribution," *IEEE Industry Applications Society 35th Annual Meeting*, vol. 5, pp. 3445-3451, 2000.

[4] M. Rico-Secades, E. L. Corominas, J. M. Alonso, J. Ribas, J. Cardesín, A. J. Calleja, J. García-García, "Complete Low Cost Two-Stage Electronic Ballast for 70W High Pressure Sodium Vapor Lamp Based on Current-Mode-Controlled Buck-Boost Inverter," *IEEE Transactions on Industry Applications*, vol.3, pp. 1841-1846, 2002.

[5] Light Research Center, Rensselaer Polytechnic Institute, "Guide to Fluorescent Lamp-Ballast Compatibility," h t t p://w w w.lrc.rpi.edu/ programs/NLPIP/PDF/VIEW/Guide1.pdf, (accessed on January 2009.)

[6] S. Ben-Yaakov, M. Shvartsas, "An Electronic Ballast for Fluorescent Lamps with no Series Passive Elements," *Applied Power Electronics Conference and Exposition,* vol.2, *pp.* 670-675, 2001.

[7] M. Polonskii, A. R. Seidel, *Reatores Eletrônicos para Iluminação Fluorescente*, 1st ed., Ijuí, RS: UNIJUÍl, 2008.

[8] J. Garcia-Garcia, J. Cardesín, J. Ribas, A. J. Calleja, M. Rico-Secades, J. M. Alonso, E. L. Corominas, "Minimization of Acoustic Resonances in HID Lamps: Analysis and Comparison of Power Harmonics Content in High Frequency non-Resonant Inverters," *IEEE Transactions on Power Electronics*, vol. 20, pp. 1467-1479, 2005.

[9] NXP Semiconductors, "AN10273 – Power MOSFET Single-Shot and Repetitive Avalanche Ruggedness Rating," March 2009.

[10] S. Ben-Yaakov, M. Shvartsas, S. Glozman, "Statics and Dynamics of Fluorescent Lamps Operating at High Frequency: Modeling and Simulation," *IEEE Transactions on Industry Applications,* pp. 1486-1492, 2002.

[11] J. Garcia-Garcia, J. Cardesin, J. Ribas, A. Calleja, E.L. Corominas, J.M. Alonso, M. Rico-Secades, "Nonresonant, Quasi-Square Wave, High-Frequency Inverter for HID Lamps Operation from a DC Bus," *38th IAS Annual Meeting,* vol.1, pp. 332-338, 2003.